Riset Geologi dan Pertambangan
(Geology and Mining Research)

RESEARCH ARTICLE
OPEN ACCESS

Riset Geologi dan Pertambangan (2025) Vol. 35, No. 2, 89–108
DOI: 10.55981/risetgeotam.2025.1390

Keywords:
Gunung Batu
Graha Puspa
pseudostatic analysis
horizontal seismic coefficient
percent water fill

Corresponding author:
wira006@brin.go.id

Article history:
Received: 24 April 2025
Revised: 16 June 2025
Accepted: 20 August 2025

Author Contributions:
Conceptualization: WC, AT, APM
Data curation: WC, IAS, IAD
Formal analysis: WC, IAD, RDK
Funding acquisition: WC, AT, APM Investigation: WC, APM, KH, HTA
Methodology: WC, IAS, AT, MRD
Supervision: IAS, AT
Visualization: WC
Writing – original draft: WC, IAS
Writing – review & editing: WC, IAS

Citation:
Cakrabuana, W., Sadisun, I. A., Tohari, A., Dinata, I.A., Daryono, M.R., Kartiko, R.D., Martireni, A.P., Hermawan, K., Atmojo, H.T., 2025. Evaluation of andesit slopes stability using pseudostatic limit equlibrium method in Lembang active fault zone, West Java, Indonesia. *Riset Geologi dan Pertambangan, 35 (2)*, 89–108, doi: 10.55981/risetgeotam.2025.1390

Evaluation of andesite slopes stability using pseudostatic limit equilibrium method in Lembang active fault zone, West Java, Indonesia

Wira Cakrabuana[1], Imam A. Sadisun[2], Adrin Tohari[1], Indra A. Dinata[2], Mudrik R. Daryono[1], Rendy D. Kartiko[2], Antonina P. Martireni[1], Koko Hermawan[1], Hasan T. Atmojo[3]

[1]Badan Riset dan Inovasi Nasional, Jl. Raya Serpong, Tangerang Selatan, Banten 15314, Indonesia
[2]Institut Teknologi Bandung, Jl. Ganesha No. 10, Bandung, Jawa Barat 40132, Indonesia
[3]Universitas Pembangunan Nasional Veteran Yogyakarta. Jl. Ring Road Utara No.104, Sleman 55283, DI Yogyakarta, Indonesia

Abstract

Earthquakes and rainfall can trigger landslides in many regions of Indonesia. Rock slopes of andesite outcrops in Gunung Batu and Graha Puspa areas coincide with the Lembang active fault zone in West Java. The region is also subjected to high-intensity rainfall. Thus, the rock slopes are prone to failure during earthquake shaking and heavy rainfall. To mitigate the hazards associated with slope failure in residential areas close to the rock slopes, it is necessary to assess the slope failure hazard at the andesite hill slopes. The study presented in this paper aims to analyse the stability of the andesite slopes using the pseudostatic limit equilibrium method and evaluate the effect of variations of regional seismicity and water content on the stability of the slopes. Pseudostatic analysis considered the peak ground acceleration (PGA) and the calculated horizontal seismic coefficient (k_h). The limit equilibrium method was focused on toppling and wedge failure cases. Based on the analysis, the andesite slopes in Gunung Batu and Graha Puspa are stable (FoS ≥ 1.1) in factual conditions (dry-static). In contrast, all slopes have the lowest FoS values (less stable-unstable) under the saturated-pseudostatic conditions. The threshold values of k_h and %w (percent water fill) for the slopes' instability were obtained by varying the regional seismicity and water content conditions. It is recommended that numerical slope stability modeling (i.e., finite element method) be conducted to improve the accuracy of the models.

1. Introduction

Earthquakes and rainfall are some of the factors that can trigger landslides (Keefer, 1984; Iverson, 2000; Sassa et al., 2007; Tatard et al., 2010). West Java is a province on Java Island, Indonesia, with a high landslide susceptibility (Sugianti et al., 2014). West Java has the potential for earthquakes, high rainfall, complex geological structures, and infrastructures with many human activities (Widiatmaka et al., 2013; Gunadi et al., 2017; Supendi et al., 2018; Soehaimi et al., 2022; Basid et al., 2024; Hadmoko et al., 2024). Reflecting on the facts, research is needed on the hazards of landslides in West Java triggered by earthquakes and rainfall factors.

The Lembang fault is an active fault about 10 km north of Bandung City, West Java (Daryono et al., 2019). This fault can potentially cause an earthquake of 6.5-7 magnitude. An earthquake of this magnitude has the potential to cause slope instability within its radius of influence. Some of the rock slopes that coincide with the Lembang active fault zone are andesite slopes located in the Gunung Batu and Graha Puspa areas, West Bandung Regency, West Java, which have moderate-high rainfall (1000-3000 mm/year) (Sundari et al., 2023). Both slopes are close to settlements and tourist attractions, so there are risk factors that need to be taken into account. According to Cakrabuana et al. (2024), the outcrops at both locations have different types of failure. The failure of Gunung Batu andesite outcrops will involve a toppling mechanism. Meanwhile, the failure of the andesite outcrops in the Graha Puspa will have the potential to be governed by both toppling and wedge failures.

This research aims to evaluate the stability of the andesite slopes in both areas against the variations of regional seismicity and water content of the slopes. The objectives of this study are to (1) analyse the stability of the andesite slopes using the pseudostatic limit equilibrium method and (2) evaluate the effect of horizontal seismic coefficient (k_h) and percent water fill (%w) on the stability of the slopes.

2. Research location

Physiographically, the area of Gunung Batu and Graha Puspa is in the Bandung zone (van Bemmelen, 1949). This zone is a depression among several mountains filled with young volcanic deposits. These two regions are in an area controlled by a west-east-oriented geological structure known as the Java pattern, which was formed about 32 million years ago (Pulunggono and Martodjojo, 1994). The Lembang fault discussed in this research is one structure that follows this pattern.

The Lembang fault is a sinistral strike-slip active fault, west-east-oriented, with a length of 29 km and located about 10 km north of Bandung City (Daryono et al., 2019). This fault slips at a rate of 1.95-3.45 mm/year and can potentially cause earthquakes of 6.5-7 magnitude and a return period of 170-670 years. Based on its geometry, the Lembang fault is divided into six sections (Figure 1). Gunung Batu area is in the Gunung Batu section, and Graha Puspa area is in the Cihideung section.

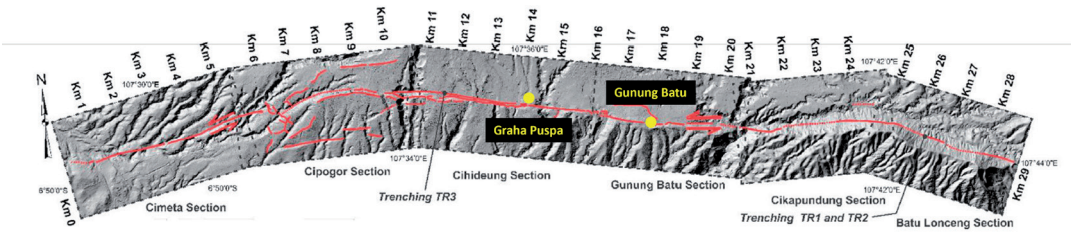

Figure 1. Map showing active fault traces and general morphology of the Lembang fault, its sections, and trenching sites (modified from Daryono et al., 2019).

Geologically, the research area is composed of a 35-20 thousand years old tuffaceous sand unit, which is characterized by a low-relief topography that is strongly eroded by the main river system (Dam, 1994; Sunardi and Kimura, 1998; Kartadinata et al., 2002; Nasution et al., 2004; Daryono et al., 2019). This unit is dominated by coarse tuffaceous sand lithology with an average thickness of 45 m, which contains fragments of igneous rock and tuff with a size of 0.5-1 cm in an open fabric. The geological map of the research area can be seen in Figure 2. The andesite slopes discussed in this research are intrusions and lava that are not mapped on the regional scale (Junursyah and Agustya, 2017; Cakrabuana et al., 2024).

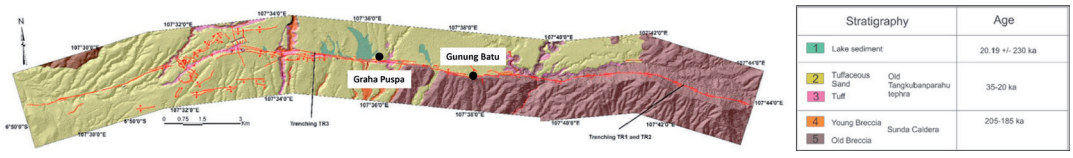

Figure 2. Map of lithological units along the Lembang fault. The table shows stratigraphic correlations with dated major geological events (modified from Dam, 1994; Sunardi and Kimura, 1998; Kartadinata et al., 2002; Nasution et al., 2004; Daryono et al., 2019).

It has been mentioned that both research sites' andesite slopes are around settlements and tourist attractions. The andesite slopes in Gunung Batu are used for rock climbing and are located around residential areas and outdoor cafes. The andesite slopes at Graha Puspa are near outdoor cafes and glamping locations. Figures 3 and 4 are satellite images and photographs showing the research location at various scales. In each area, three slopes were studied, namely GB-01, GB-02, and GB-03 in Gunung Batu and GP-01, GP-02, and GP-03 in Graha Puspa.

Figure 3. Satellite image and photographs showing the Gunung Batu area.

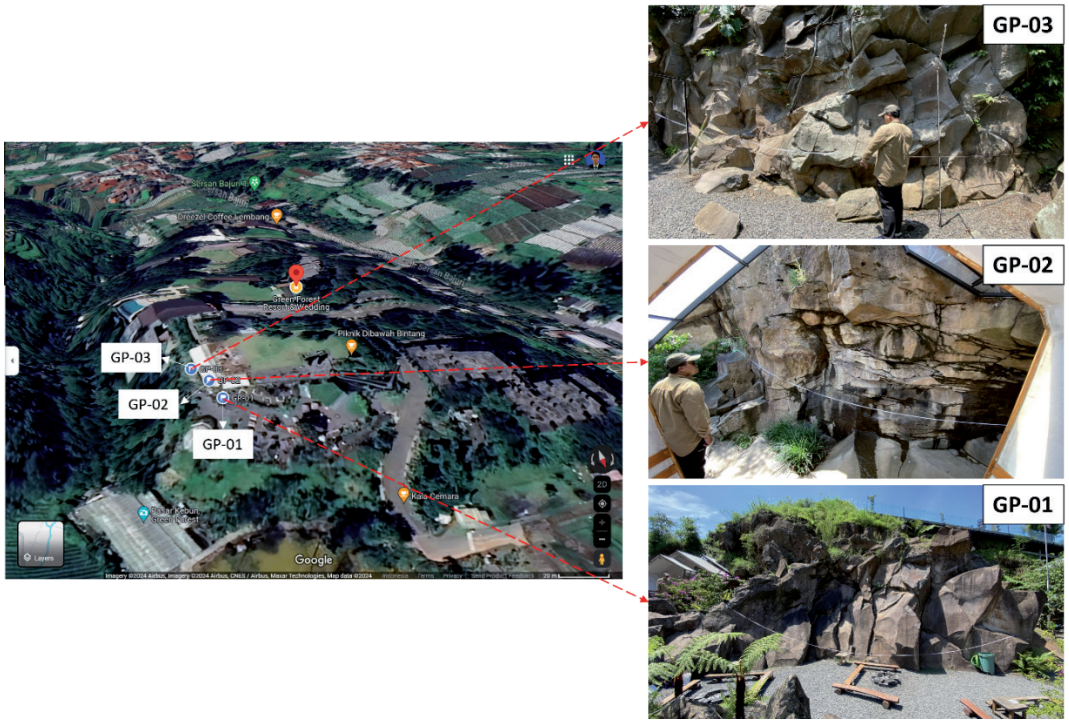

Figure 4. Satellite image and photographs showing the Graha Puspa area.

3. Methods

Before analysing and evaluating the slope stability in the software, a literature study on the pseudostatic and limit equilibrium methods was carried out.

Pseudostatic method

In addition to gravitational force, one of the causes of landslides is earthquakes (Widisaputra et al., 2020). Landslides triggered by earthquakes have not received much attention in Indonesia (Utomo, 2008). The type of landslides produced can be creeping or giant debris avalanches. Earthquakes can provide vibration/pressure on mineral particles and weak parts of rock and soil masses so that slope stability is disturbed (Sutiyono et al., 2017).

Several active faults potentially cause earthquakes in West Java, which increases the risk of landslides. The earthquake wave can be amplified or deamplified when it travels through the soil layer, causing an increase or decrease in the peak acceleration on the ground surface (PGA). This seismic acceleration must be included in the pseudostatic slope stability analysis to calculate the safety factor accurately. In such an analysis, the seismic loading is modelled as a statically applied inertial force (Gurudeo and Digambar, 2017). The formulas for calculating the safety factor in the pseudo-static method are given in Equations 1-3.

$$F_h = \frac{a_h.W}{g} = k_h.W \quad (1)$$

$$F_v = \frac{a_v.W}{g} = k_v.W \quad (2)$$

$$FoS = \frac{resisting\ moment}{static+pseudostatic\ driving\ moment} = \frac{c.L+[(W-F_v).cos\beta-F_h.sin\beta].tan\phi}{(W-F_v).sin\beta+F_h.cos\beta} \quad (3)$$

Where:
F_h = horizontal seismic force (N)
F_v = vertical seismic force (N)
a_h = horizontal seismic acceleration (m/s^2)
a_v = vertical seismic acceleration (m/s^2)
k_h = horizontal seismic coefficient (gal)
k_v = vertical seismic coefficient (gal)
W = weight force (N)
g = gravitational acceleration (m/s^2)
FoS = factor of safety
c = cohesion (Pa)
L = length of the failure plane (m)
ϕ = internal friction angle (°)
β = slope dip (°)

Based on SNI 8460:2017 (BSN, 2017), the designed earthquake is determined with the probability of exceedance during the planned life of 50 years, which is 10% or equivalent to a return period of 475 years. The minimum safety factor required for pseudostatic analysis is greater than 1.1 using the horizontal seismic coefficient (k_h) obtained from half of the PGA of the site. Since both study areas are geologically made up of andesite outcrops, the site class of the study area can be classified as S_B (bedrock). Consequently, the PGA amplification factor used is 1 (BSN, 2017). It is also assumed that this case study's vertical seismic coefficient (k_v) is very small, so that it can be ignored.

Limit equilibrium method

According to SNI 8460:2017, slope stability analysis using the limit equilibrium method is based on predicting slope failure types. In Cakrabuana et al. (2024), it has been understood that the slopes of GB-01, GB-02, GB-03, GP-02, and GP-03 have the potential to experience toppling failure, while the GP-01 slope has the potential to experience wedge failure. In this study, the slope stability analysis uses *RocTopple* software for toppling failure cases and *SWedge* software for wedge failure cases (Rocscience, 2002).

The limit equilibrium method in this research case of toppling failure is limited to simple cases using a basic understanding of the factors that cause toppling failure (Goodman and Bray, 1976). Stability analysis uses an iterative process that considers the dimensions of all rock blocks and the forces acting on them. The stability of each block is determined, starting from the top block. Each block can become stable, topple, or slide. The overall slope is considered unstable if the bottom block slides or topples. The basic condition required for the analysis is that the friction angle at the base of each block is greater than the dip of the base plane, so that sliding in the base plane does not occur if there is no external force acting on the slope. The limit equilibrium method is well-suited to account for external forces acting on the slope, which can then be used to simulate various factual conditions in the field. Various illustrations explaining the principle of limit equilibrium in the case of toppling failure can be seen in Figure 5.

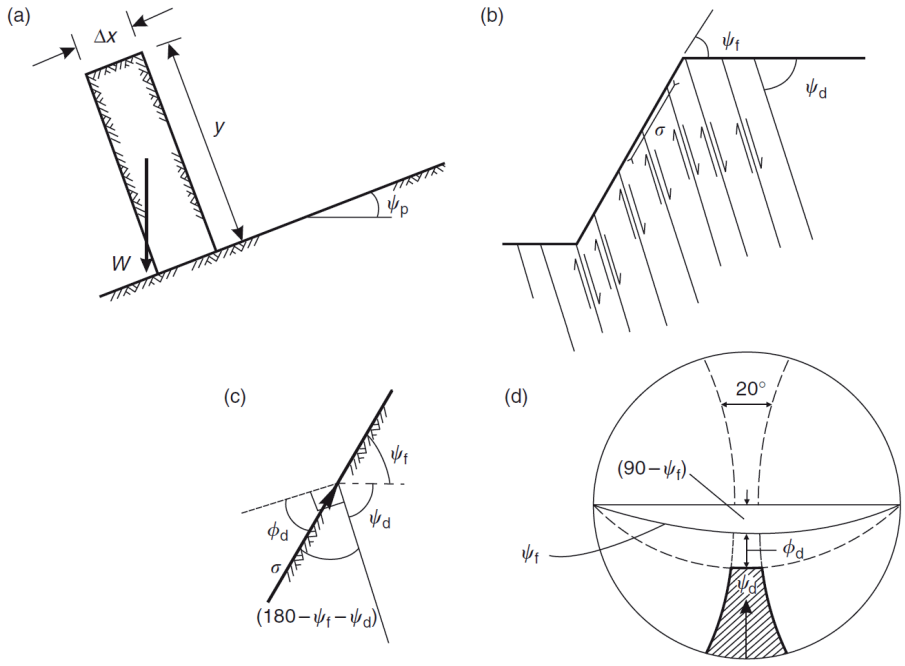

Figure 5. Kinematic conditions for flexural sliding before toppling failure (Wyllie and Mah, 2004): (a) block shape test; (b) the direction of stress and sliding on the rock slope; (c) conditions for inter-layer slip; (d) compilation of the kinematics test of toppling failure on a stereoplot.

The safety factor (FoS) in wedge failure is defined in Equation 4 (Wyllie and Mah, 2004). The FoS was made based on the assumption that the failure was caused only by friction and that both sliding surface friction angles (ϕ) were equally significant. R_A and R_B are the normal reactions on the planes of A and B. W sin ψ_i is the gravitational force acting in the direction of the intersection line. R_A and R_B are determined by considering them as normal and parallel components to the direction of the intersection. The internal friction angle used in the FoS calculation in the case of wedge and toppling failures is the friction angle of discontinuity (BSN, 2017). Various illustrations explaining the principle of limit equilibrium in the case of wedge failure can be seen in Figure 6.

$$FoS = \frac{(R_A + R_B)\tan\phi}{W \sin\psi_i} \quad (4)$$

Where:
FoS = factor of safety
R_A = reaction of normal force on plane A (N)
R_B = reaction of normal force on plane B (N)
ϕ = internal friction angle (°)
W = weight force (N)
ψ_i = plunge of discontinuity intersection (°)

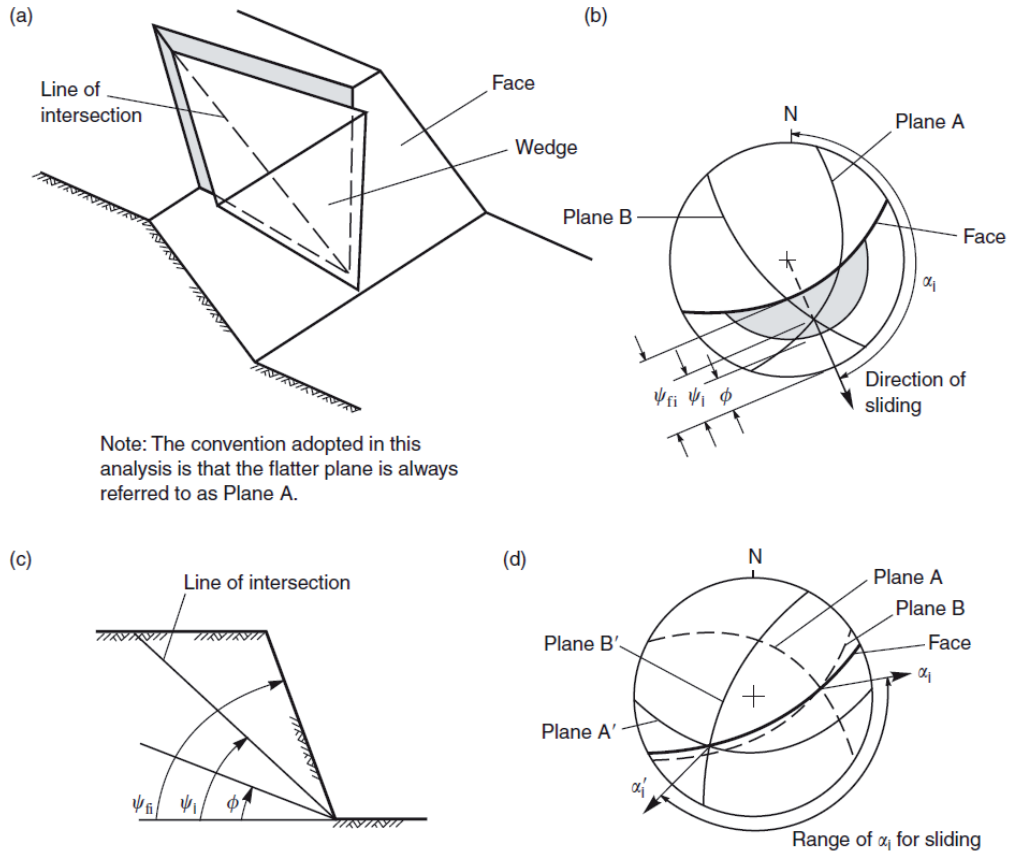

Figure 6. Geometric conditions for wedge failure (Wyllie and Mah, 2004): (a) illustration of the geometry of wedge failure; (b) a stereoplot showing the intersection lines and plunge ranges that allow a wedge failure to occur; (c) the display of the slope at the angle of the intersection; (d) a stereoplot showing the trend range of intersecting lines that allow a wedge failure to occur.

4. Results and discussion

This section contains the results of the analysis of the earthquake influence using the pseudostatic method, the slope stability analysis using the limit equilibrium method, the evaluation of slope stability using several variations in seismicity and water content, and the determination of the threshold values of the k_h and %w parameters at both study locations. As elaborated in the previous section, horizontal seismic coefficient (k_h) is horizontal seismic acceleration (a_h) divided by gravitational acceleration (g), while percent water fill (%w) is the percentage of water content in the rock mass discontinuity.

Earthquake influence analysis

Since the study locations are ≤ 10 km from the Lembang Fault, it is not allowed to use the PGA value generated from probabilistic seismic hazard analysis (PSHA) for pseudostatic slope stability analysis (PusGen, 2017). The PGA value must be generated from the deterministic seismic hazard analysis (DSHA) or site-specific procedure. This study determined the PGA value empirically through a literature study. Hussain et al. (2023) made PGA maps of Bandung Raya (Figure 7) based on the earthquake geology study by Daryono et al. (2019). The PGA maps are created in two magnitude scenarios, 6.6 for the minimum and 7.0 for the maximum. The return period applied is 170-670 years.

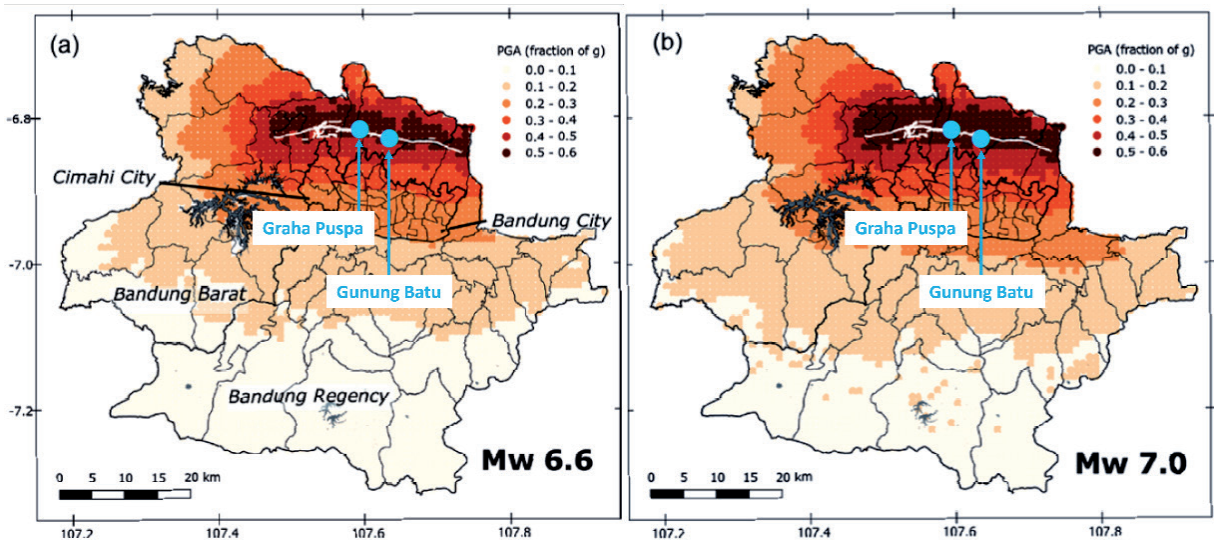

Figure 7: The median ground motion fields (modified from Hussain et al., 2023) for magnitude 6.6 (a) and magnitude 7.0 (b) scenarios. The blue dots indicate the study locations. The white line shows the Lembang Fault. Peak ground acceleration (PGA) is expressed in fractions.

Based on the provisions of SNI 8460:2017 (BSN, 2017), the return period used for pseudostatic slope stability analysis is 475 years. In this case, the assumption is that the PGA map with a 425-year return period is considered equivalent to the PGA map with a 7.0 magnitude scenario. The PGA map with a 7.0 magnitude shows that the two research sites have a PGA value range of 0.5-0.6 g. In this study, the maximum value was 0.6 g, and the calculated k_h for the two locations was 0.3 g.

Slope stability analysis

Tables 1 and 2 list the parameters entered in the *RocTopple* and *SWedge* software. In the *RocTopple* software are included slope-related parameters (dip, height); toppling joints (spacing, dip), a dip of the base plane; the unit weight of the rock; Barton-Bandis parameters of toppling joints, including joint roughness coefficient (JRC), joint wall compressive strength (JCS), and residual friction angle of discontinuity (ϕ_r); seismic coefficient; and water pressure. In the *SWedge* software, parameters almost similar to *RocTopple* are included; only the discontinuity used here is two, and it is necessary to enter their dip directions.

Table 1. Slope model parameters for toppling failure.

Slope	Failure Type	Slope		Toppling Joints		Overall Base Inclination (°)	Rock Unit Weight (MN/m³)	Base Joint			Toppling Joint			Horizontal Seismic Coefficient (g)	Water Pressure	
		Dip (°)	Height (m)	Spacing (m)	Dip (°)			JRC	JCS (MPa)	ϕ_r (°)	JRC	JCS (MPa)	ϕ_r (°)		% Fill	Water Unit Weight (MN/m³)
GB-01	Toppling	67	12	0.38	85	57	0.0257	13.6	143.27	25	13.6	143.27	25	0	0	0.00981
GB-02	Toppling	72	12	0.4	66	48	0.0257	13.26	143.27	25	13.26	143.27	25	0	0	0.00981
GB-03	Toppling	81	12	0.27	27	72	0.0257	12.18	143.27	25	12.18	143.27	25	0	0	0.00981
GP-02	Toppling	75	5	0.27	4	73	0.02605	14.38	157.27	25	14.38	157.27	25	0	0	0.00981
GP-03	Toppling	70	5	0.37	79	64	0.02605	15	157.27	25	15	157.27	25	0	0	0.00981

Table 2. Slope model parameters for wedge failure.

Slope	Failure Type	Slope				Rock Unit Weight (MN/m³)	Joint 1					Joint 2					Horizontal Seismic Coefficient (g)	Water Pressure	
		Dip (°)	Dip Direction (°)	Height (m)	Length (m)		Dip (°)	Dip Direction (°)	JRC	JCS (MPa)	ϕ_r (°)	Dip (°)	Dip Direction (°)	JRC	JCS (MPa)	ϕ_r (°)		% Fill	Water Unit Weight (MN/m³)
GP-01	Wedge	80	30	5	11.65	0.02605	43	85	14.85	157.27	25	49	38	14.85	157.27	25	0	0	0.00981

The three Barton-Bandis parameters above are determined empirically. JRC is taken from the average JRC ratings from the scanline survey (Ulusay and Hudson, 2007). JCS is equated with the UCS value of the intact rocks that make up the slope (Barton and Choubey, 1977). ϕ_r is obtained from the estimated value of ϕ_r in the Ja parameter table (Barton, 2002). Although empirically obtained, these parameters are quite reliable and widely used by geotechnical experts as they have been tested with samples of different types of rocks around the world.

At this stage, the stability of the slope is determined by factual conditions, dry and static. The results of the GB-01 slope stability modeling showed a very high FoS value, which was 25. Almost all of the parts of the GB-01 slope are very stable, except for the slope foot, which has the potential to experience sliding. The slopes of GB-02 and GB-03 have FoS values of 1.928 and 1.404. Both slopes are in stable condition (FoS ≥ 1.1), but there is potential for toppling almost throughout the slope and slight sliding at the foot of the slope. The results of slope stability modelling in the Gunung Batu area can be seen in Figures 8-10.

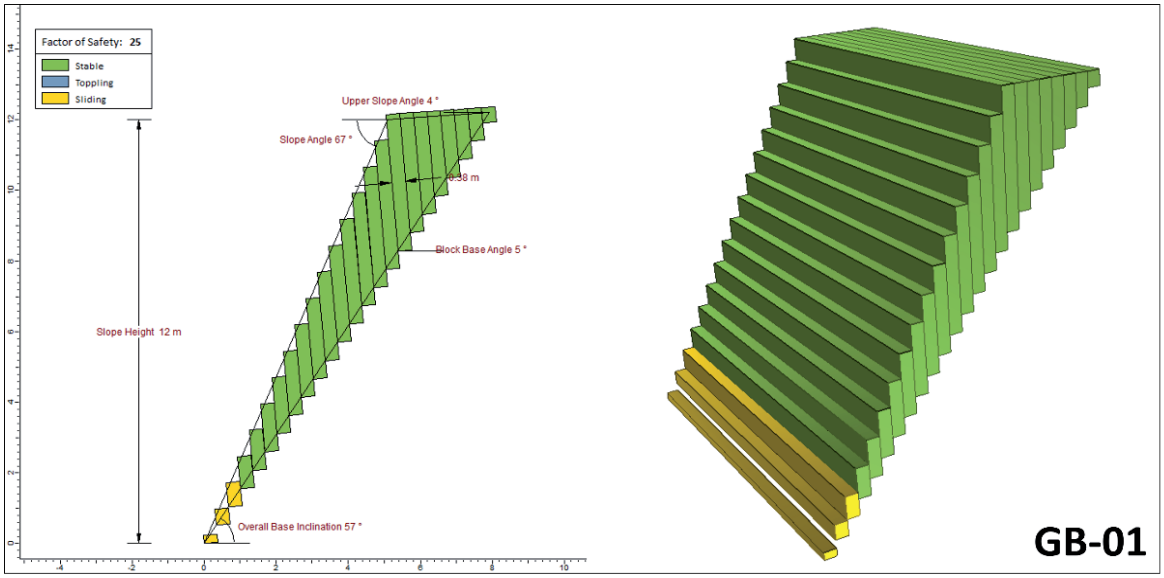

Figure 8. Results of modelling the stability of the GB-01 slope under factual (dry-static) conditions.

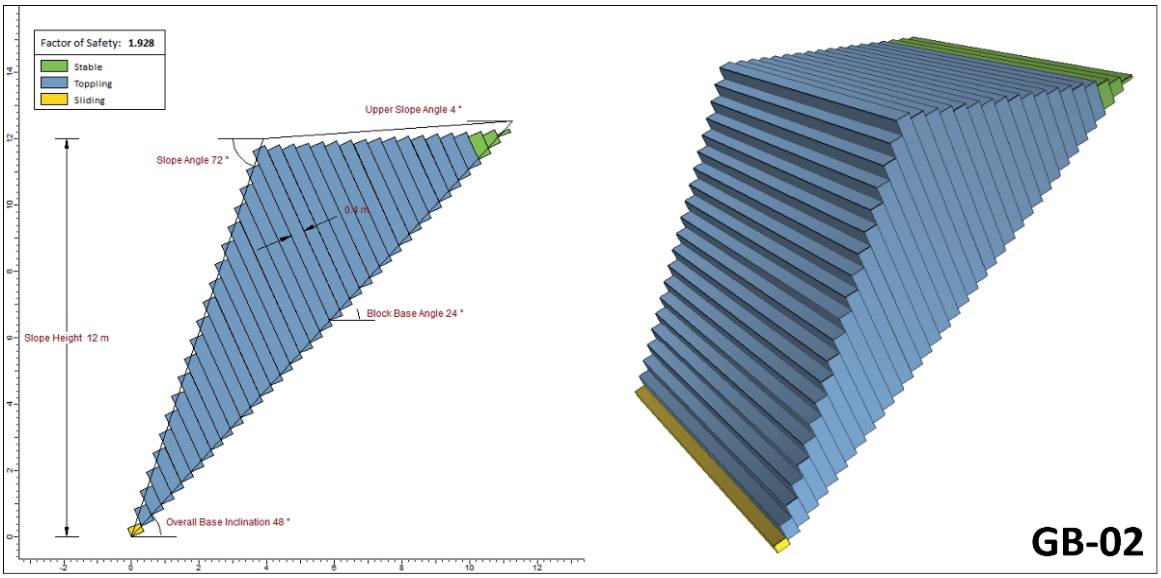

Figure 9. Results of modelling the stability of the GB-02 slope under factual (dry-static) conditions.

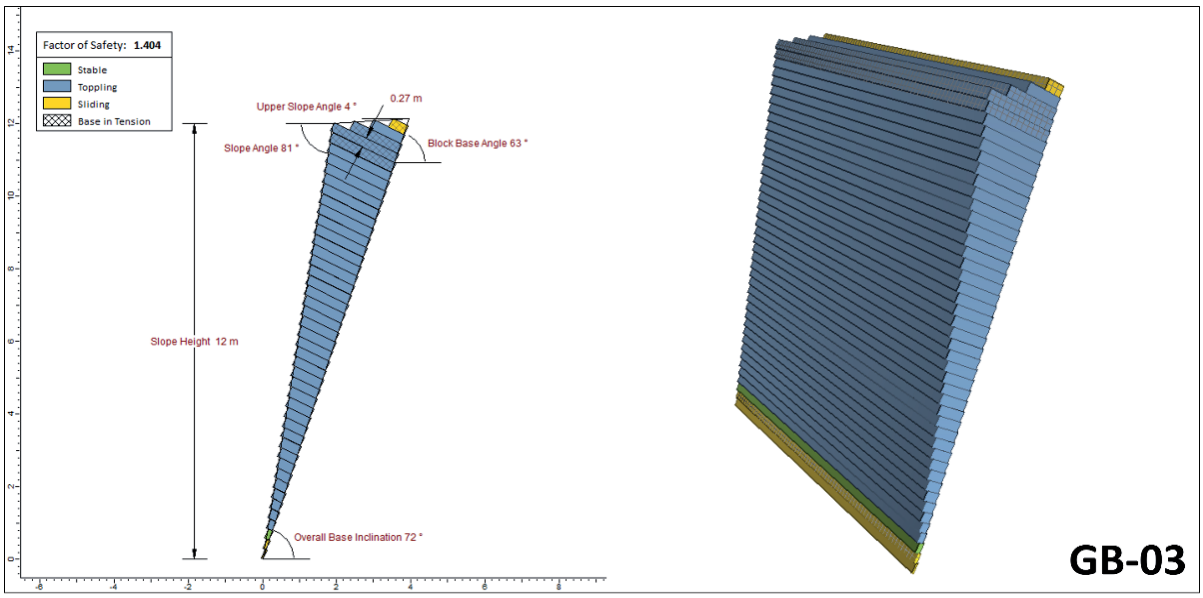

Figure 10. Results of modelling the stability of the GB-03 slope under factual (dry-static) conditions.

Through stability modeling in *SWedge*, the GP-01 slope was found to be stable with a FoS of 2.3883. The wedge failure that potentially occurs in GP-01 is shaped like the tip of an arrow that crosses horizontally on a slope. The *RocTopple* software system rejects the GP-02 slope. The slope cannot be modelled for its failure because the toppling joint dip is very low. Just like the case of GB-01, the GP-03 slope has a very high FoS, which is 14.135. The top of the GP-03 slope is stable, while the bottom has the potential to slide. The results of slope stability modelling in the Graha Puspa area can be seen in Figures 11-13.

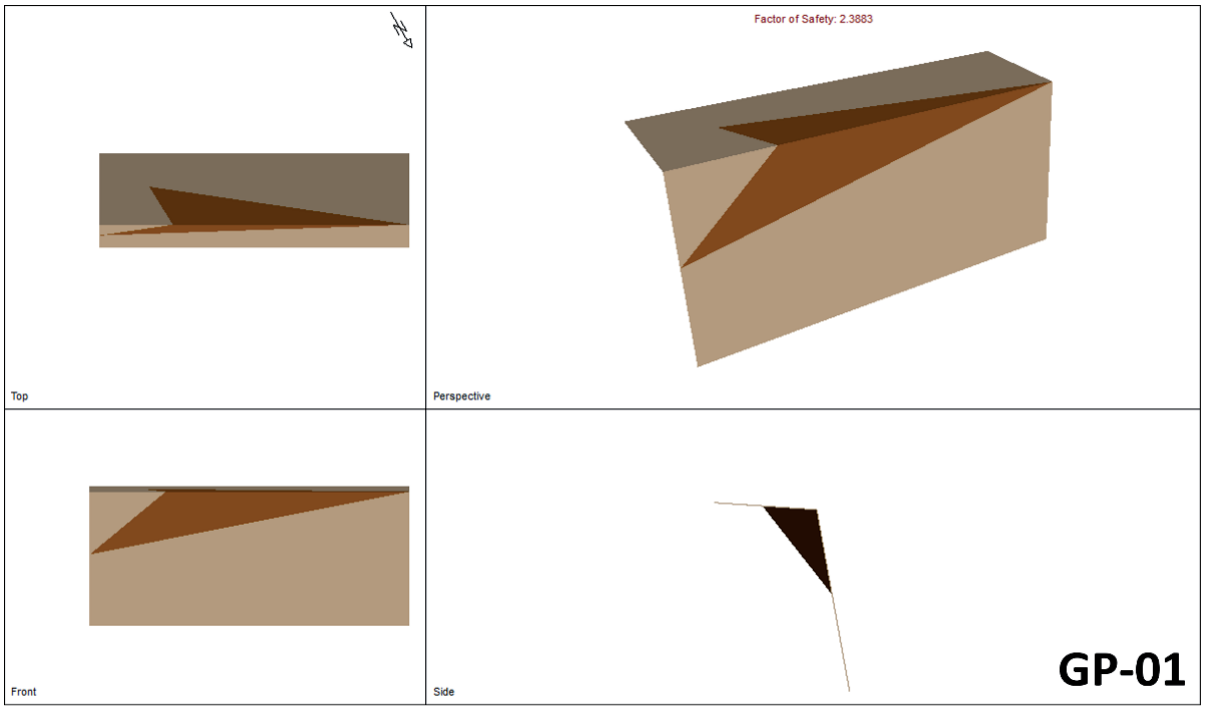

Figure 11. Results of modelling the stability of the GP-01 slope under factual (dry-static) conditions.

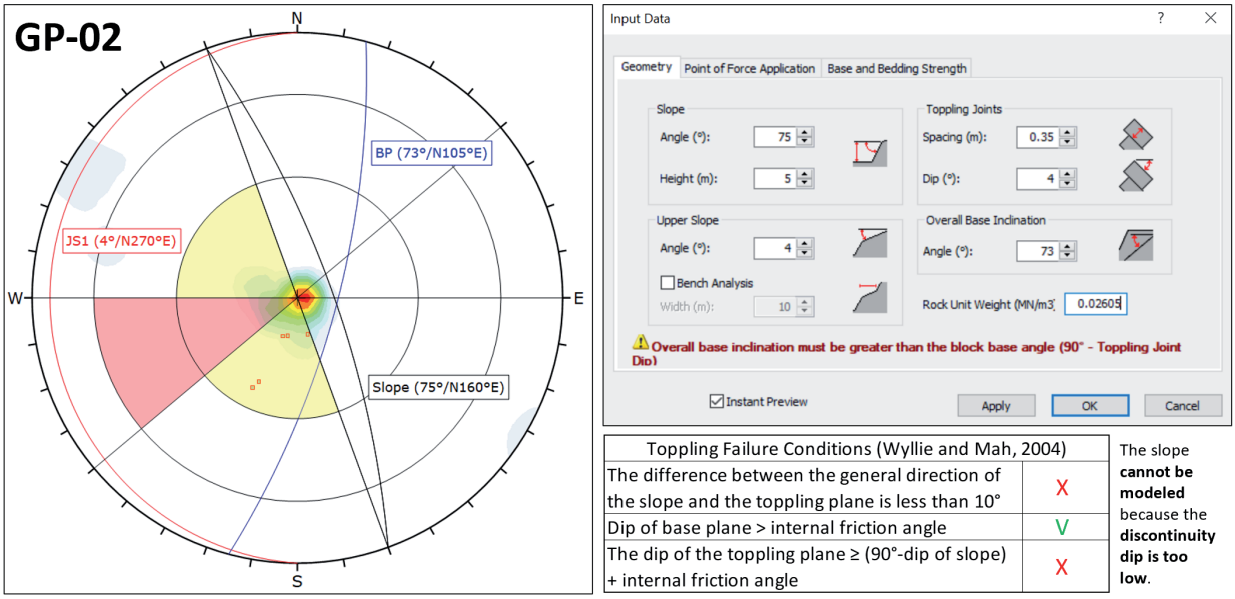

Toppling Failure Conditions (Wyllie and Mah, 2004)	
The difference between the general direction of the slope and the toppling plane is less than 10°	X
Dip of base plane > internal friction angle	V
The dip of the toppling plane ≥ (90°-dip of slope) + internal friction angle	X

The slope **cannot be modeled** because the **discontinuity dip is too low**.

Figure 12. Screenshot of the toppling failure modelling software for the GP-02 slope case.

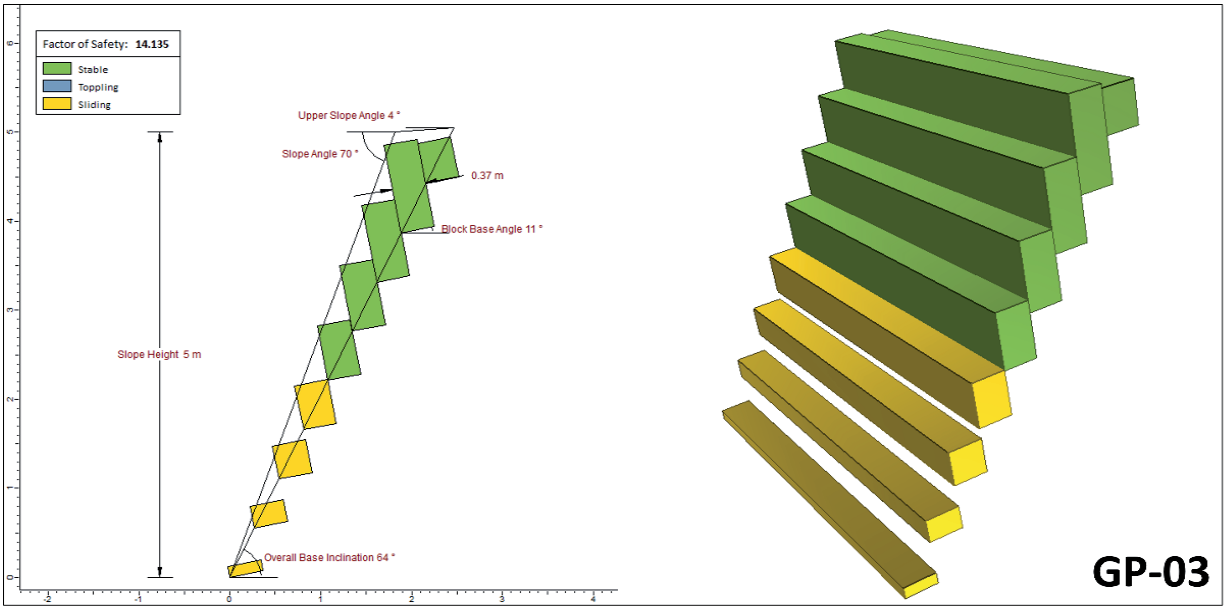

Figure 13. Results of modelling the stability of the GP-03 slope under factual (dry-static) conditions.

In factual conditions (dry and static), all slopes are in a stable/safe condition (FoS ≥ 1.1). The GB-01 and GP-03 slopes have a very high FoS because the discontinuity configuration favours slope stability in this condition. This is shown in the sensitivity curves of the toppling joint dips of the two slopes (Figures 14 and 15). In the case of the GB-01 slope, the FoS experienced a drastic increase in the toppling joint dip range of 82-84° (FoS 2 to 25). The toppling joint dip included in the modelling is 85°, so the GB-01 slope has an FoS of 25. In the case of the GP-03 slope, the FoS experienced a drastic increase in the toppling joint dip range of 71-84° (FoS 8 to 25). The toppling joint dip included in the modelling is 79°, so the GP-03 slope has an FoS of 14s.

Slope stability evaluation

Subsequently, the five slopes are modelled with seismicity and water content variations. Slopes are varied by conditions: saturated-pseudostatic (%w=100, k_h=0.3 g), saturated-static (%w=100, k_h=0 g), dry-pseudostatic (%w=0, k_h=0.3 g), and dry-static (%w=0, k_h=0 g). Almost all slopes tend to increase FoS in that sequence of variations. This means that almost all slopes are more susceptible to failure by water than by earthquakes.

The results of the slope stability modelling with variations in seismicity and water content conditions for slopes in the Gunung Batu area can be seen in Figures 16-18. All slopes show an increasing trend of FoS except GB-03 (Figure 19). Under dry-pseudostatic conditions, the sensitivity curves of the k_h and %w parameters of the three slopes are shown in Figure 20. The curve shows that on the GB-01 and GB-02 slopes, FoS has a downward trend as k_h and %w increase. This trend was not found on the GB-03 slope; the sensitivity curve showed an irregular pattern, so the slope did not experience an increase in FoS like the other two slopes when varied with the order of the conditions as above. This makes GB-03 the most susceptible slope to failure in Gunung Batu.

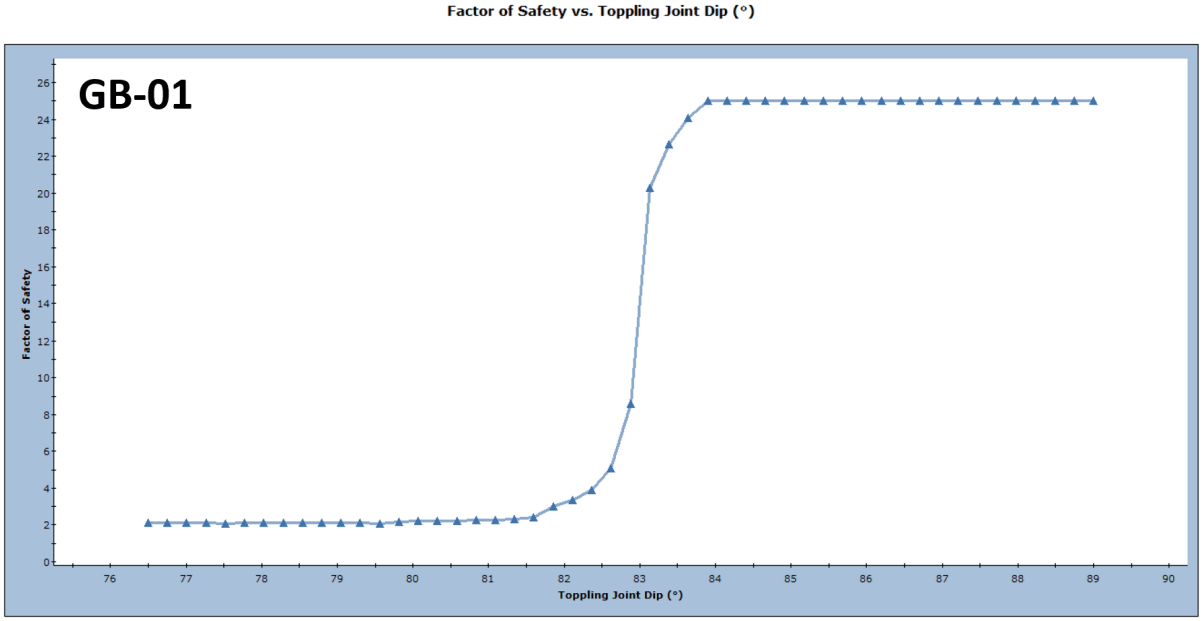

Figure 14. Sensitivity curve of the toppling joint dip on the GB-01 slope case (dry-static conditions).

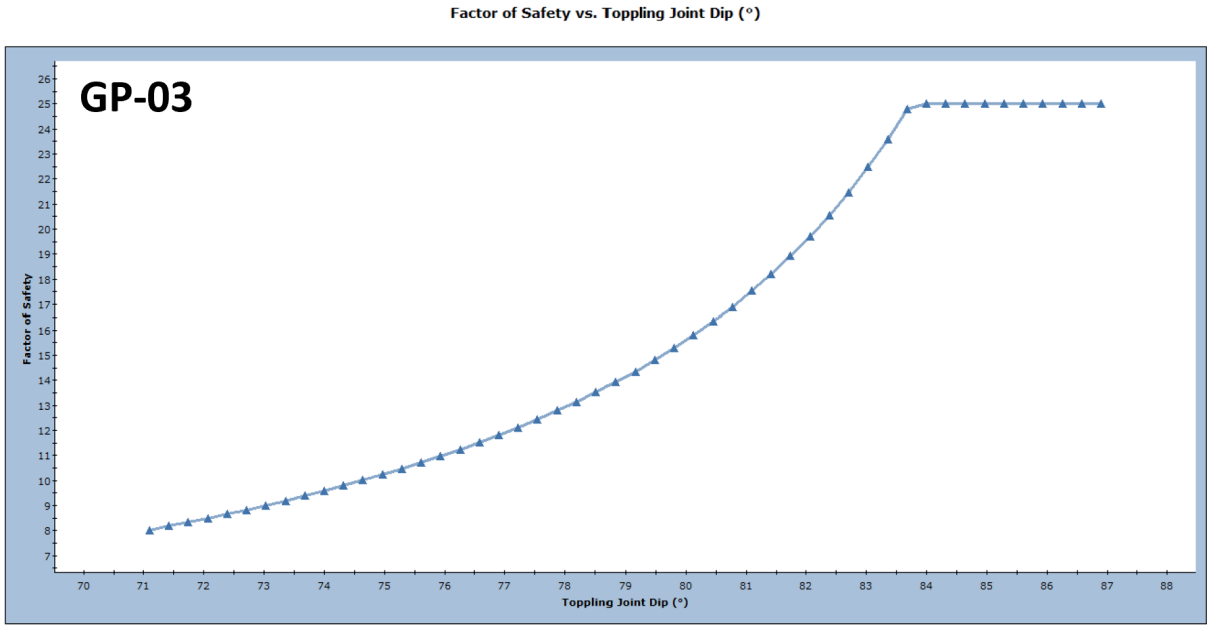

Figure 15. Sensitivity curve of the toppling joint dip on the GP-03 slope case (dry-static conditions).

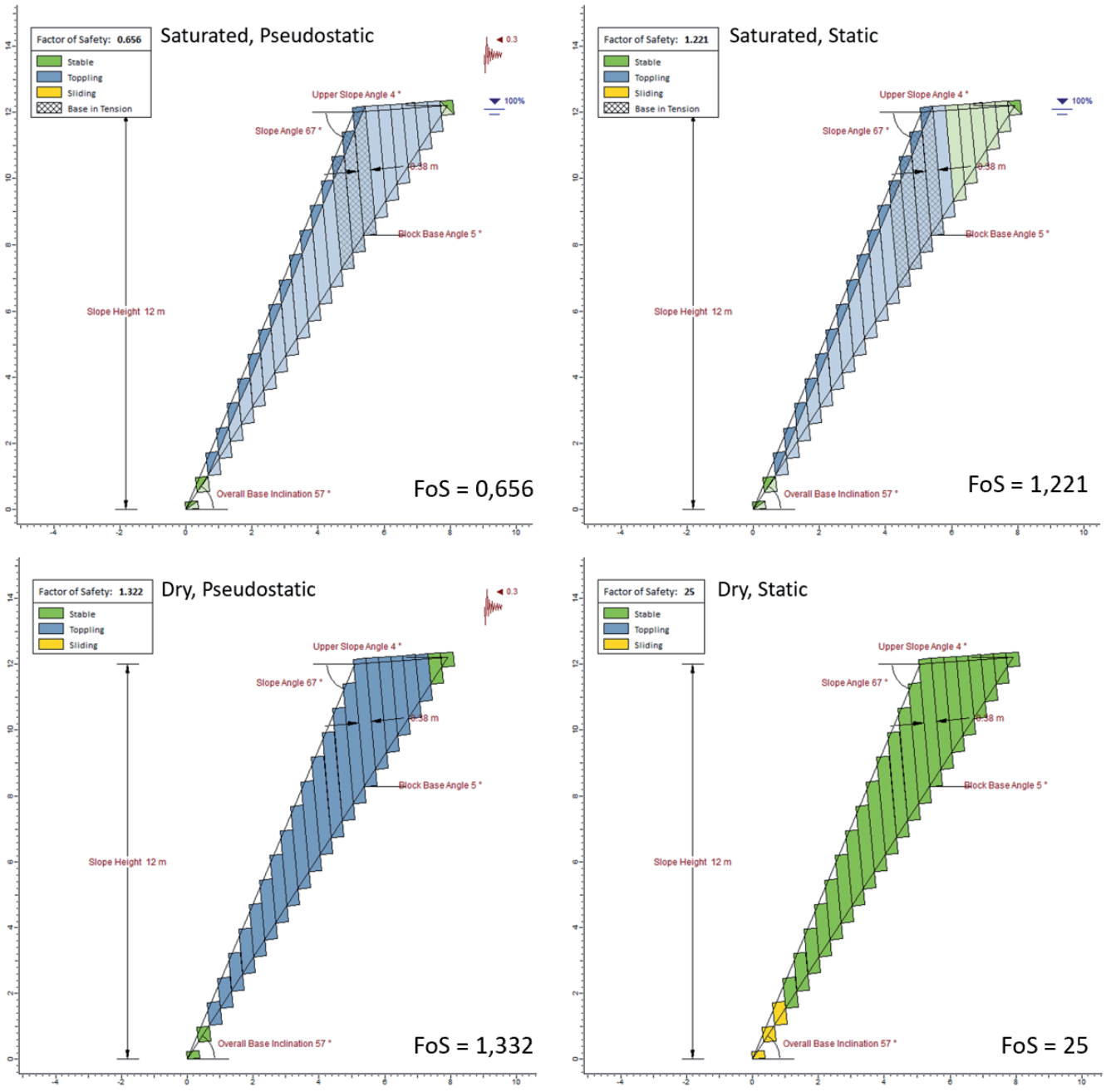

Figure 16. Results of modelling the stability of the GB-01 slope with variations in seismicity and water content conditions.

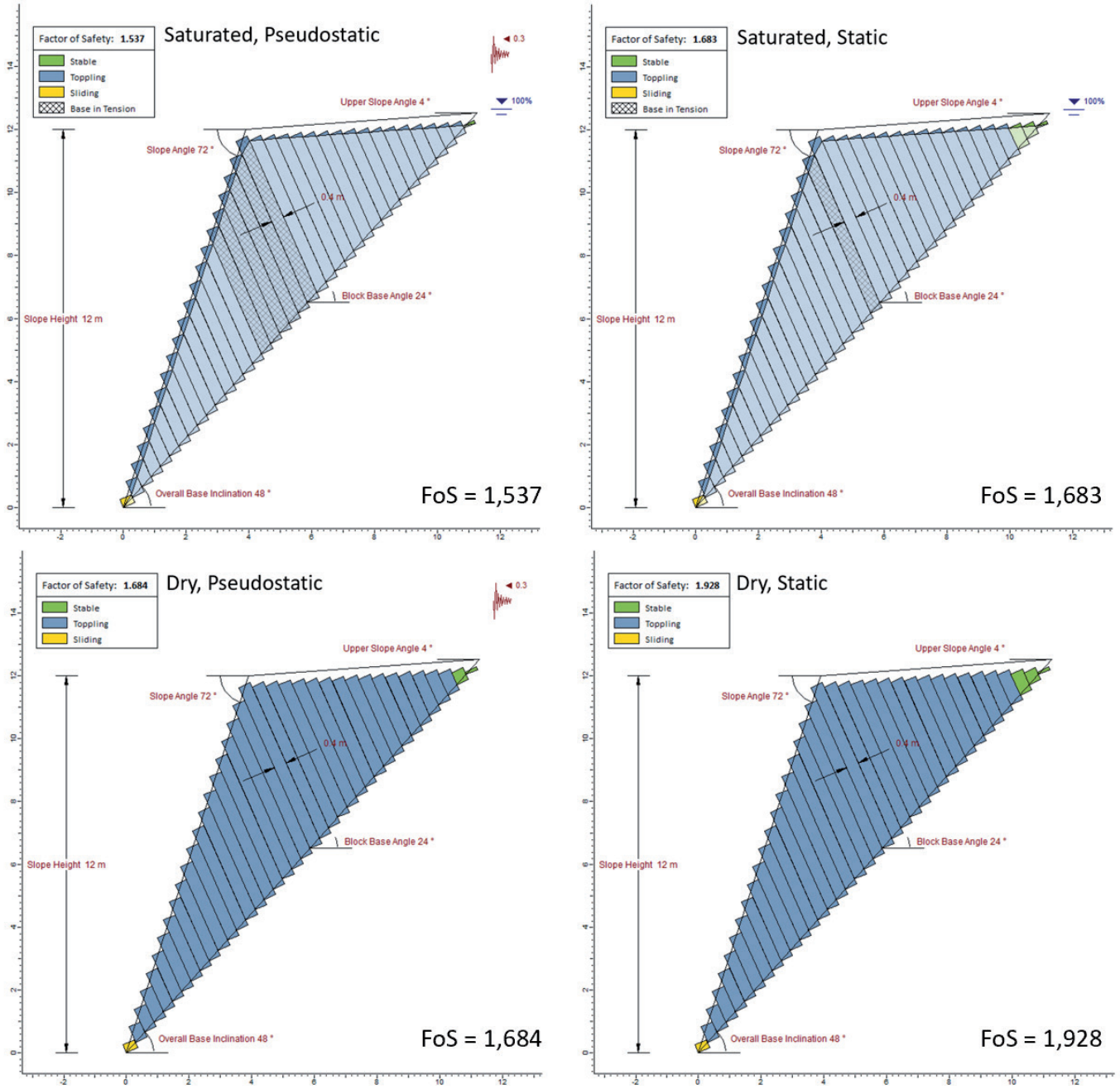

Figure 17. Results of modelling the stability of the GB-02 slope with variations in seismicity and water content conditions.

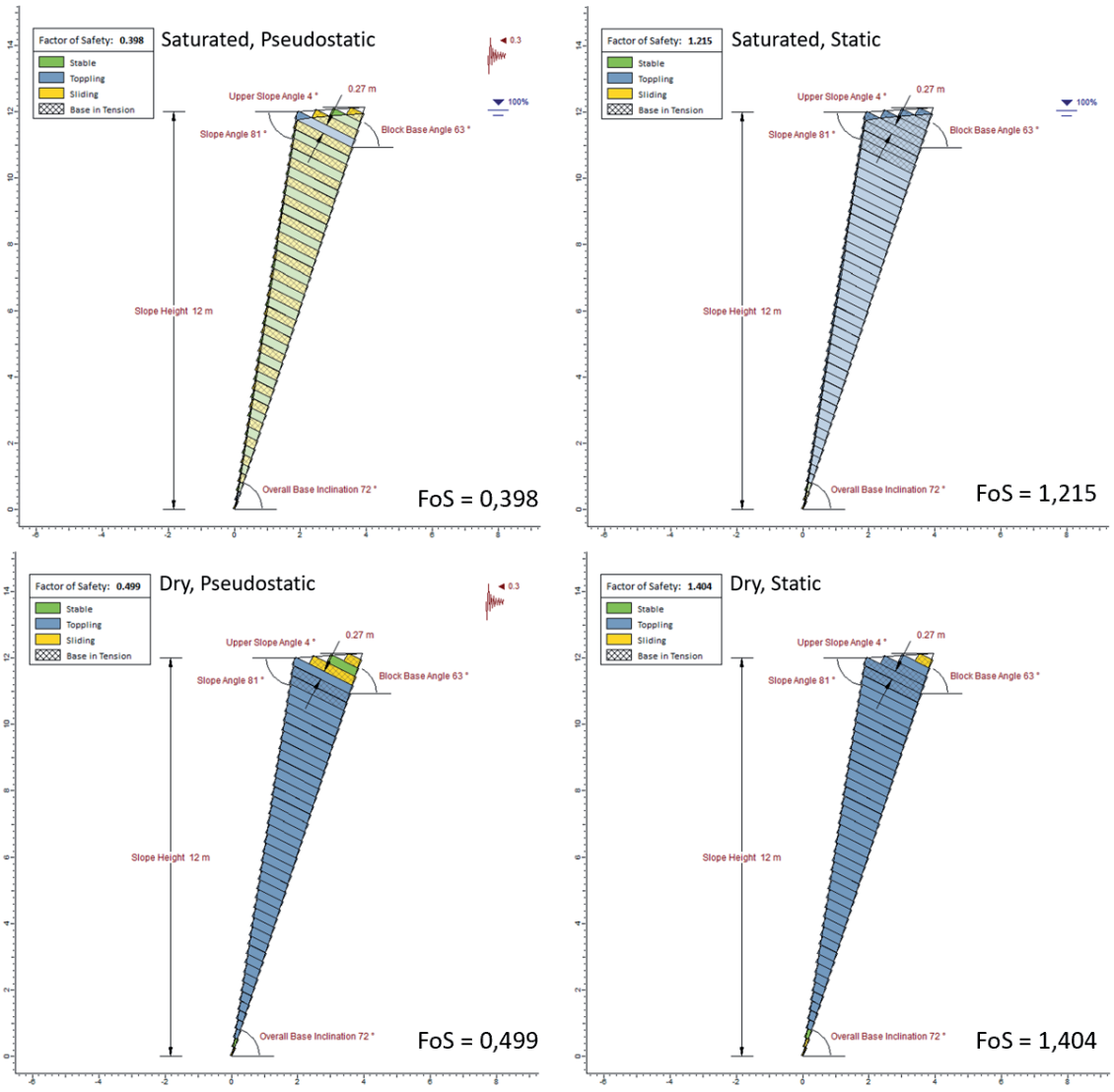

Figure 18. Results of modelling the stability of the GB-03 slope with variations in seismicity and water content conditions.

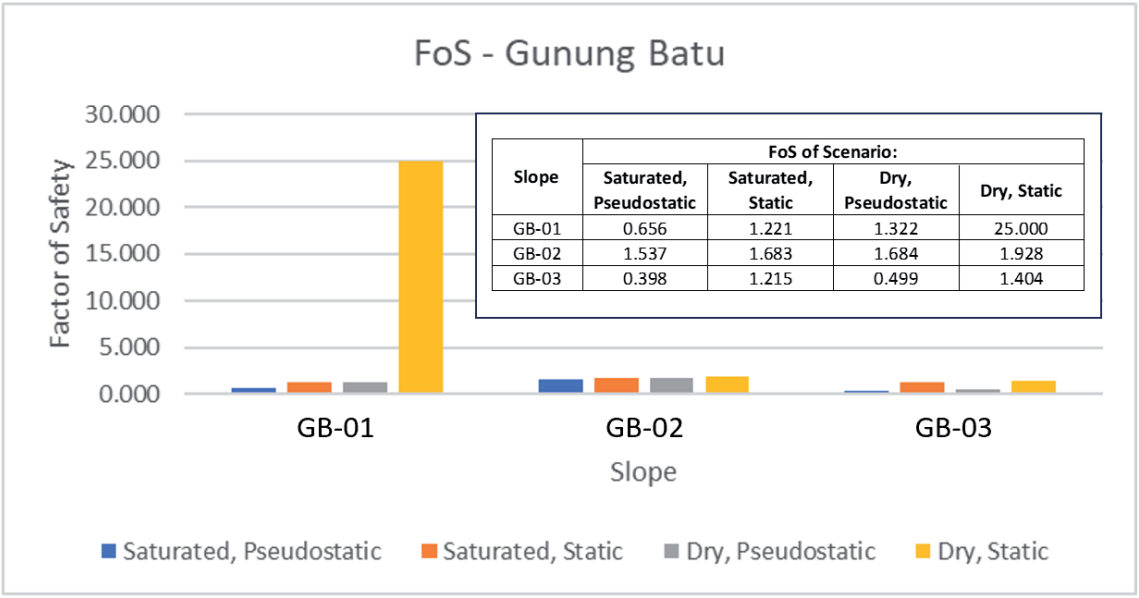

Slope	FoS of Scenario:			
	Saturated, Pseudostatic	Saturated, Static	Dry, Pseudostatic	Dry, Static
GB-01	0.656	1.221	1.322	25.000
GB-02	1.537	1.683	1.684	1.928
GB-03	0.398	1.215	0.499	1.404

Figure 19. Comparison of FoS values of GB-01, GB-02, and GB-03 slopes with variations in seismicity and water content conditions.

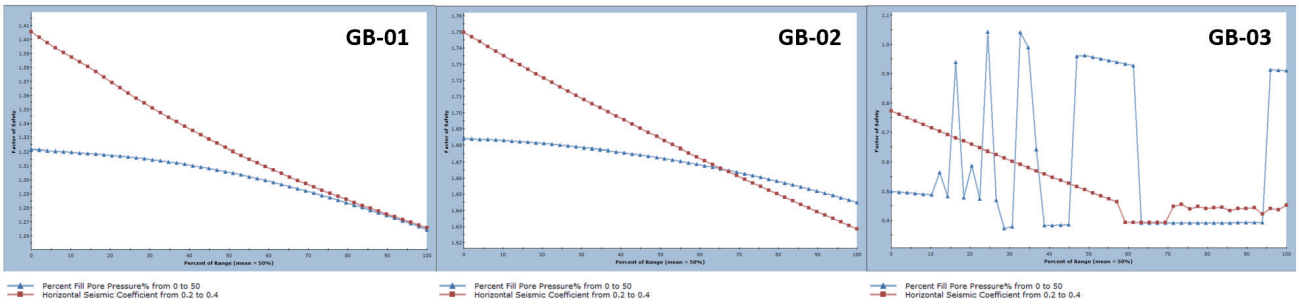

Figure 20. Comparison of the sensitivity curves of k_h and %w parameters on the GB-01, GB-02, and GB-03 slopes (dry-pseudostatic conditions).

The results of the slope stability modelling with variations in seismicity and water content conditions for slopes in the Graha Puspa area can be seen in Figures 21 and 22. All slopes show an increasing trend of FoS when varied with the order of the conditions as above (Figure 23).

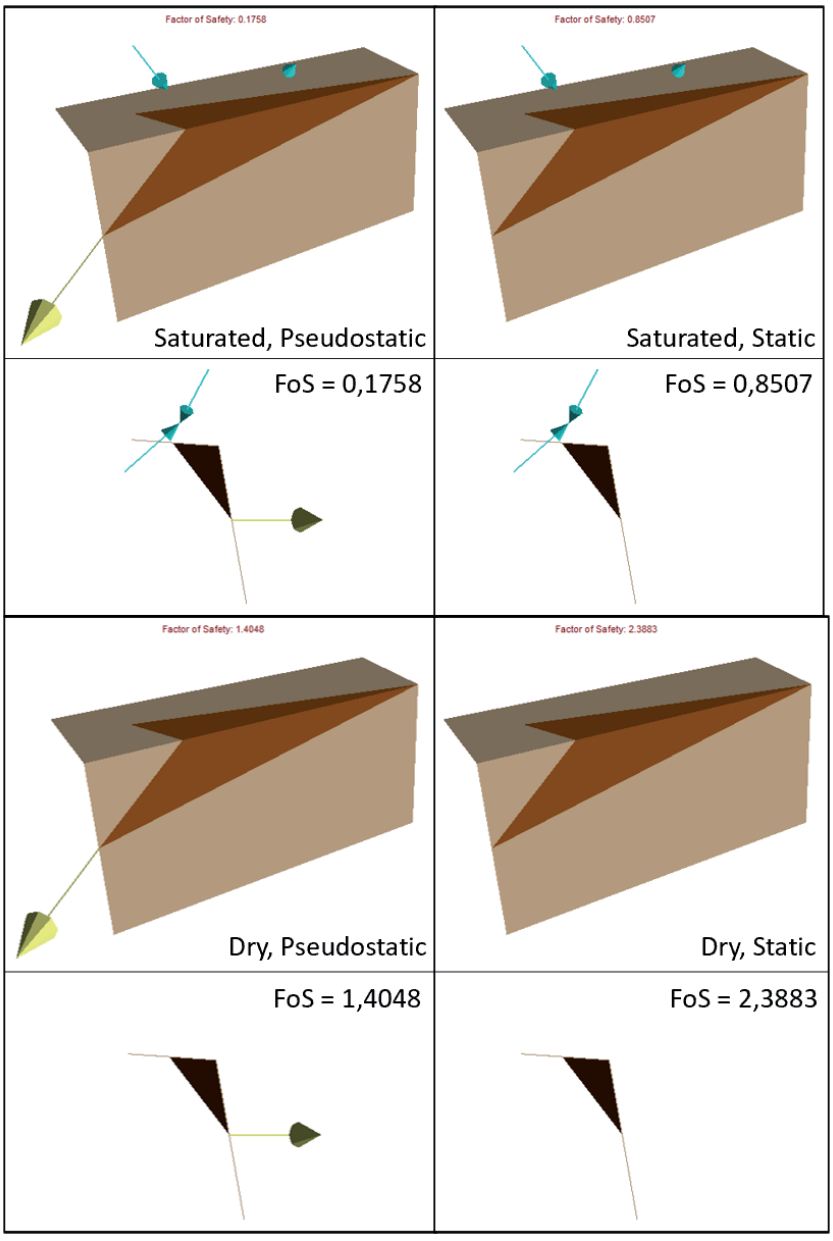

Figure 21. Results of modelling the stability of the GP-01 slope with variations in seismicity and water content conditions.

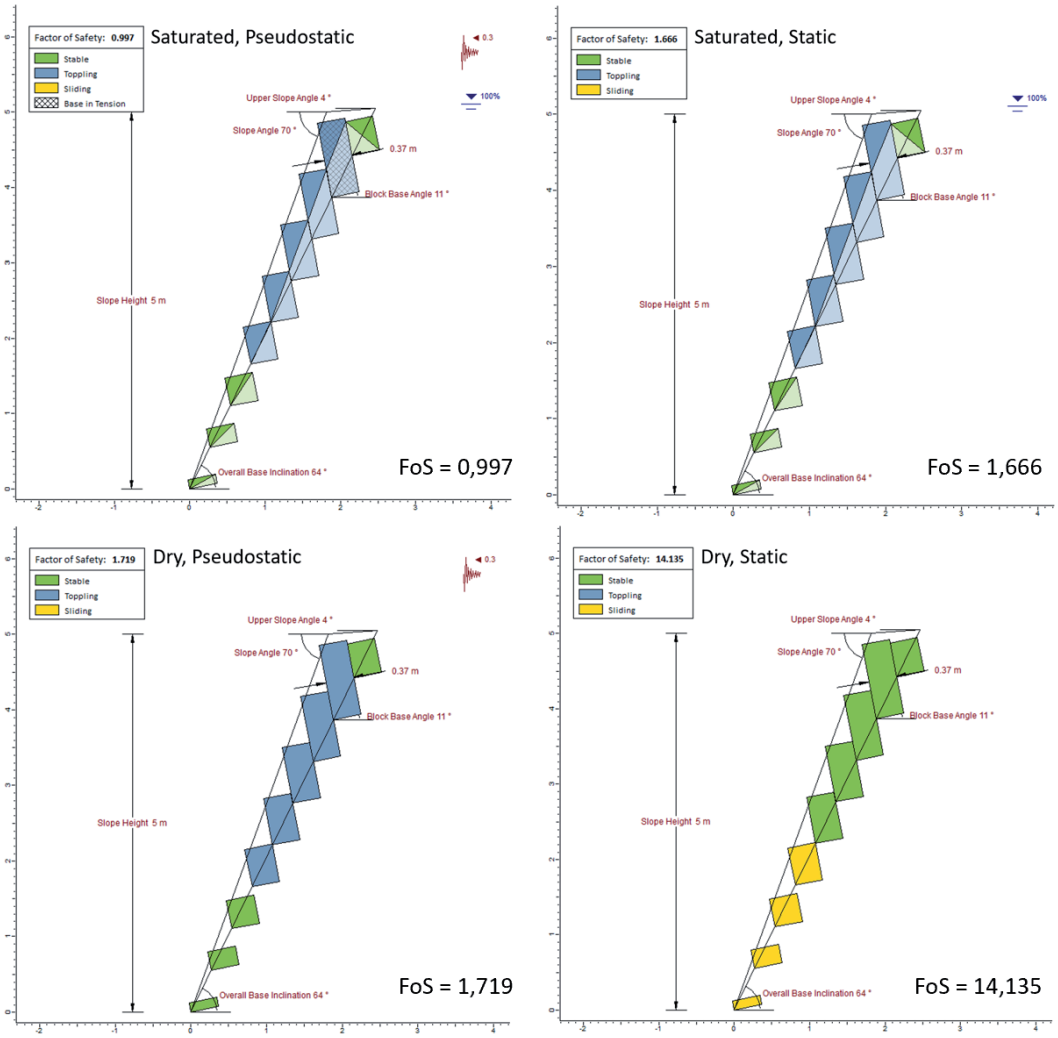

Figure 22. Results of modelling the stability of the GP-03 slope with variations in seismicity and water content conditions.

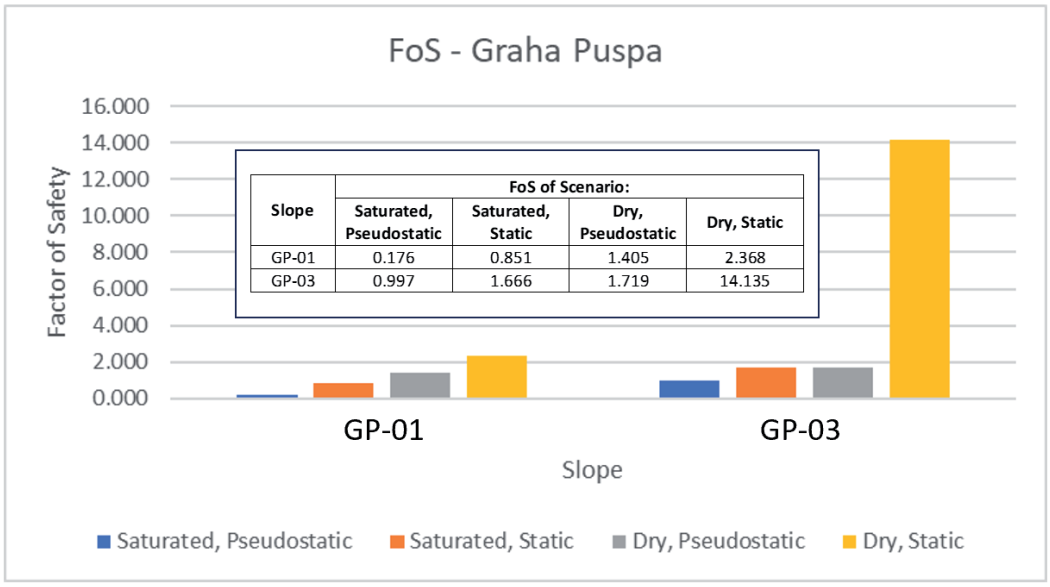

Slope	FoS of Scenario:			
	Saturated, Pseudostatic	Saturated, Static	Dry, Pseudostatic	Dry, Static
GP-01	0.176	0.851	1.405	2.368
GP-03	0.997	1.666	1.719	14.135

Figure 23. Comparison of FoS values of GP-01 and GP-03 slopes with variations in seismicity and water content conditions.

Determination of k_h and %w threshold values

Based on the seismic coefficient and water pressure parameters, the threshold values of k_h and %w are determined in various conditions. The k_h threshold values are determined on three water content conditions variations, namely %w = 0, 50, and 100. The %w threshold values are determined on three variations of seismicity conditions: k_h = 0 g, 0.15 g, and 0.3 g.

At %w = 0, the GB-01 and GB-02 slopes are stable, while the GB-03 slope is unstable at $k_h \geq 0.175$ g. At %w = 50, the GB-01 and GB-02 slopes are stable, while the GB-03 slope is unstable at $k_h \geq 0.15$ g. At %w = 100, the GB-02 slope is stable; the GB-01 and GB-03 slopes are unstable at $k_h \geq 0.08$ g and 0.05 g. Under this condition, the sensitivity of k_h to GB-03 FoS begins to decrease at k_h = 0.075 g. The determination of the k_h threshold values for the andesite slopes in Gunung Batu can be seen in Figure 24.

At k_h = 0 g, the GB-01, GB-02, and GB-03 slopes are stable. At k_h = 0.15 g, the GB-02 slope is stable, the GB-03 slope is completely unstable, and the GB-01 slope is unstable at %w ≥ 92. At k_h = 0.3 g, the GB-02 slope is stable, the GB-03 slope is completely unstable, and the GB-01 slope is unstable at %w ≥ 70. At k_h = 0.15 g and 0.3 g, GB-03 %w has no sensitivity to FoS. The determination of the %w threshold values for the andesite slopes in Gunung Batu can be seen in Figure 25.

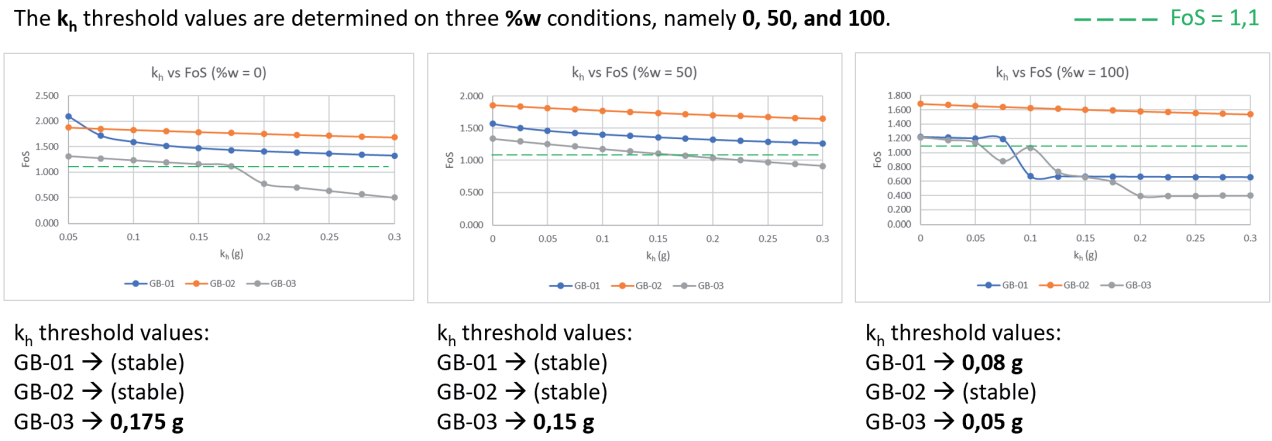

Figure 24. The determination of k_h threshold values in Gunung Batu.

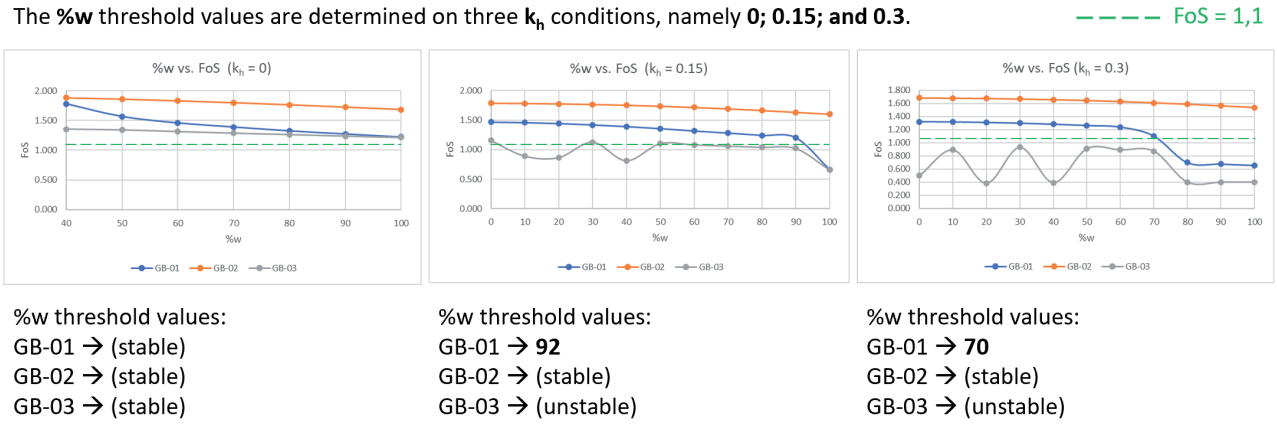

Figure 25. The determination of %w threshold values in Gunung Batu.

At %w = 0 and 50, the GP-01 and GP-03 slopes are stable. At %w = 100, the GP-01 slope is completely unstable, and the GP-03 slope is unstable at $k_h \geq 0.09$ g. Under this condition, the sensitivity of k_h to GP-03 FoS begins to decrease at k_h = 0.2 g. The determination of the k_h threshold values for the andesite slopes in Graha Puspa can be seen in Figure 26.

At k_h = 0 g, the GP-03 slope is stable, and the GP-01 slope is unstable at %w ≥ 93. At k_h = 0.15 g, the GP-01 and GP-03 slopes are unstable at %w ≥ 80 and 88. At k_h = 0.3 g, the GP-01 and GP-03 slopes are unstable at %w ≥ 60 and 58. Under this condition, the sensitivity of %w to GP-03 FoS decreases at %w = 70. The determination of the %w threshold values for the andesite slopes in Graha Puspa can be seen in Figure 27.

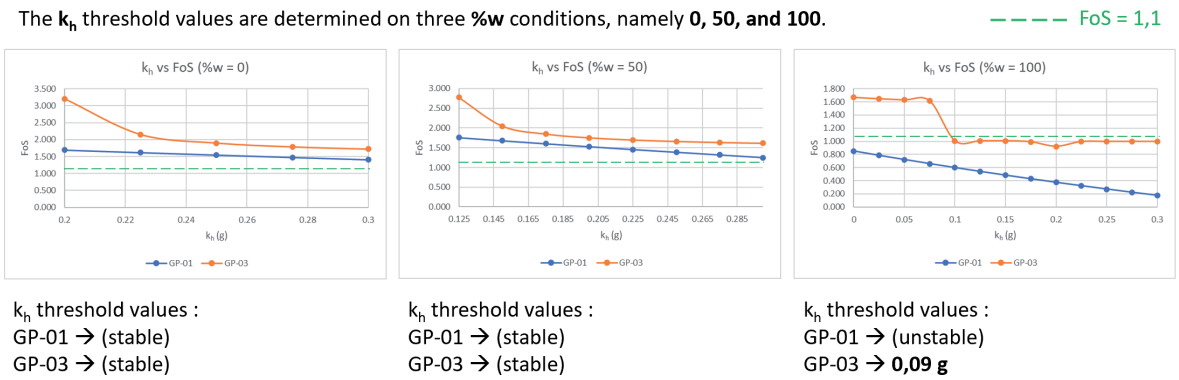

Figure 26. The determination of k_h threshold values in Graha Puspa.

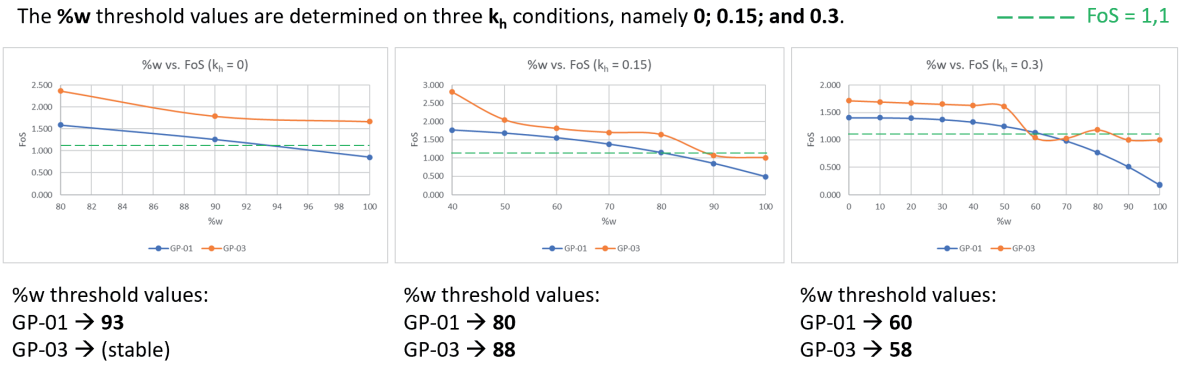

Figure 27. The determination of %w threshold values in Graha Puspa.

5. Conclusions

In factual conditions (dry-static), all andesite slopes in Gunung Batu and Graha Puspa are in a stable condition (FoS ≥ 1.1). Except for the GB-02 slope, the FoS of most of the slopes generally decreases more significantly under saturated-pseudostatic conditions, indicating the slope is sensitive to changes in k_h and %w. The extreme increase in FoS on the slopes of GB-01 and GP-03 is because of a favourable discontinuity configuration for the slope stability.

Based on the pseudostatic analysis of the Gunung Batu andesite slopes with an overall base inclination higher than 50°, the dry rock slopes will be prone to toppling failure during an earthquake with a PGA higher than 0.35 g. Meanwhile, the wet rock slopes only require a PGA higher than 0.1 g to fail in the same case.

Considering the difference in failure types of the andesite slopes in the Graha Puspa site, the rock slopes with wedge failure potential are more prone to failure than those of toppling failure under static conditions when the saturation is close to 100%. Under the pseudostatic condition, the wet rock slopes in the Graha Puspa site will prove to be prone to toppling failure when the earthquake produces a PGA of higher than 0.18 g.

Additional data (more scanline surveys and laboratory testing results of the slopes' rock mass) is recommended to improve the accuracy of the models in this study. Three-dimensional numerical slope stability modelling (i.e., finite element method) of the andesite rock slopes in both sites may assist in understanding the deformation that will occur during earthquake and/or rainfall and evaluate the risk of slope failure in the residential areas.

Acknowledgements

The authors would like to thank Lembaga Pengelola Dana Pendidikan (LPDP) for funding the research written in this article. The authors are grateful to Badan Riset dan Inovasi Nasional (BRIN) for helping implement this research from beginning to end. The authors also thank the Institut Teknologi Bandung (ITB) for permitting the use of licensed software in this research.

References

Barton, N., 2002. Some new Q-value correlations to assist in site characterisation and tunnel design. Int. J. Rock Mech. Min. Sci. 39, 185–216. https://doi.org/10.1016/S1365-1609(02)00011-4

Barton, N., Choubey, V., 1977. The shear strength of rock joints in theory and practice. Rock Mech. 10, 1–54. https://doi.org/10.1007/BF01261801

Basid, A., Maharani, F.A.P., Rusli, R., 2024. Analysis of Fault Patterns That Cause Destructive Earthquakes in Mainland West Java. J. Neutrino J. Fis. dan Apl. 17, 23–28. https://doi.org/10.18860/neu.v17i1.29408

BSN, 2017. SNI 8460:2017 Persyaratan Perancangan Geoteknik. Badan Standardisasi Nasional, Jakarta.

Cakrabuana, W., Sadisun, I.A., Tohari, A., Dinata, I.A., Martireni, A.P., Mahmud, H.Z., Nareswari, R.B., Hermawan, K., Atmojo, H.T., 2024. Andesite Slope Stability Analysis Using Rock Mass Rating (RMR) and Slope Mass Rating (SMR) in Gunung Batu and Graha Puspa Areas, West Bandung Regency, West Java, Indonesia. Rud. Zb. 39, 137–150. https://doi.org/10.17794/rgn.2024.4.11

Dam, M.A.C., 1994. The Late Quaternary Evolution of the Bandung Basin, West Java, Indonesia. Vrije Universitet.

Daryono, M.R., Natawidjaja, D.H., Sapiie, B., Cummins, P., 2019. Earthquake Geology of the Lembang Fault, West Java, Indonesia. Tectonophysics 751, 180–191. https://doi.org/10.1016/j.tecto.2018.12.014

Goodman, R.E., Bray, J.W., 1976. Toppling of rock slopes, in: Proceedings Specialty Conference on Rock Engineering for Foundations and Slopes. ASCE, Colorado, pp. 201–234.

Gunadi, D.S.A., Jaya, I.N.S., Tjahjono, B., 2017. Spatial Modeling of Landslide Susceptibility (Case Study In West Java Province, Indonesia). Indones. J. Electr. Eng. Comput. Sci. 5, 139–146. https://doi.org/10.11591/ijeecs.v5.i1.pp139-146

Gurudeo, C.A., Digambar, M.R., 2017. Pseudostatic Slope Stability Analysis, in: National Conference on Innovative Trends in Engineering & Technology 2017. pp. 80–83.

Hadmoko, D.S., Wibowo, S.B., Sianipar, D.S.J., Daryono, D., Fathoni, M.N., Pratiwi, R.S., Haryono, E., Lavigne, F., 2024. Co-seismic deformation and related hazards associated with the 2022 Mw 5.6 Cianjur earthquake in West Java, Indonesia: insights from combined seismological analysis, DInSAR, and geomorphological investigations. Geoenvironmental Disasters 11, 20. https://doi.org/10.1186/s40677-024-00277-6

Hussain, E., Gunawan, E., Hanifa, N.R., Zahro, Q., 2023. The seismic hazard from the Lembang Fault, Indonesia, derived from InSAR and GNSS data. Nat. Hazards Earth Syst. Sci. 23, 3185–3197. https://doi.org/10.5194/nhess-23-3185-2023

Iverson, R.M., 2000. Landslide triggering by rain infiltration. Water Resour. Res. 36, 1897–1910. https://doi.org/10.1029/2000WR900090

Junursyah, G.M.L., Agustya, G., 2017. Penafsiran Struktur Geologi di Daerah Gunung Batu Lembang Berdasarkan Korelasi Data Permukaan, Tahanan Jenis, dan Geomagnetik. J. Geol. dan Sumberd. Miner. 18, 171–182. https://doi.org/10.33332/jgsm.geologi.v18i3.332

Kartadinata, M.N., Okuno, M., Nakamura, T., Kobayashi, T., 2002. Eruptive history of Tangkuban Perahu Volcano, West Java, Indonesia: a preliminary report. J. Geog. 111, 404–409. https://doi.org/10.5026/jgeography.111.3_404

Keefer, D.K., 1984. Landslides caused by earthquakes. Geol. Soc. Am. Bull. 95, 406–421. https://doi.org/10.1130/0016-7606(1984)95<406:LCBE>2.0.CO;2

Nasution, A., Kartadinata, M.N., Kobayashi, T., Siregar, D., Sutaningsih, E., Hadisantono, R., Kadarstia, E., 2004. Geology, Age Dating and Geochemistry of the Tangkuban Parahu Geothermal Area, West Java, Indonesia. J. Geotherm. Res. Soc. Japan 26, 285–303. https://doi.org/10.11367/grsj1979.26.285

Pulunggono, A., Martodjojo, S., 1994. Perubahan tektonik Paleogen – Neogen merupakan peristiwa terpenting di Jawa, in: Prosiding Geologi Dan Geotektonik Pulau Jawa. Yogyakarta, pp. 37–50.

PusGen, 2017. Peta Sumber dan Bahaya Gempa Indonesia Tahun 2017. Jakarta.

Rocscience, 2002. Dips User's Guide - Plotting, Analysis and Presentation of Structural Data Using Spherical Projection Techniques.

Sassa, K., Fukuoka, H., Wang, F., Wang, G., 2007. Landslides induced by a combined effect of earthquake and rainfall, in: Progress in Landslide Science. pp. 193–207. https://doi.org/10.1007/978-3-540-70965-7_14

Soehaimi, A., Saputra, S.E.A., Sopyan, Y., Tanjung, R.A., Komalasari, R., Setiawan, S.P.A., 2022. Seismic Hazard Microzonation of Tasikmalaya City, West Java Province, Indonesia. Earth Sci. 11, 220–231. https://doi.org/10.11648/j.earth.20221104.18

Sugianti, K., Mulyadi, D., Sarah, D., 2014. Klasifikasi Tingkat Kerentanan Gerakan Tanah Daerah Sumedang Selatan Menggunakan Metode Storie. J. Ris. Geol. dan Pertamb. 24, 93–104. https://doi.org/10.14203/risetgeotam2014.v24.86

Sunardi, E., Kimura, J., 1998. Temporal chemical variations in late Cenozoic volcanic rocks around The Bandung Basin, West Java, Indonesia. J. Mineral. Petrol. Econ. Geol. 93, 103–128. https://doi.org/10.2465/ganko.93.103

Sundari, Y., Asdak, C., Dwiratna, S., 2023. Analisis Karakteristik Fisik Kondisi Lahan di Kabupaten Bandung Barat, in: Prosiding Seminar Nasional Pembangunan Dan Pendidikan Vokasi Pertanian. Politeknik Pembangunan Pertanian Manokwari, Manokwari, pp. 629–635. https://doi.org/10.47687/snppvp.v4i1.686

Supendi, P., Nugraha, A.N., Puspito, N.T., Widiyantoro, S., Daryono, D., 2018. Identification of active faults in West Java, Indonesia, based on earthquake hypocenter determination, relocation, and focal mechanism analysis. Geosci. Lett. 5, 10. https://doi.org/10.1186/s40562-018-0130-y

Sutiyono, D.I., Balamba, S., Sarajar, A.N., 2017. Analisis Stabilitas Lereng Akibat Gempa Di Ruas Jalan Noongan - Pangu. Tekno 15, 1–12.

Tatard, L., Grasso, J.R., Helmstetter, A., Garambois, S., 2010. Characterization and comparison of landslide triggering in different tectonic and climatic settings. J. Geophys. Res. Earth Surf. 115. https://doi.org/10.1029/2009JF001624

Ulusay, R., Hudson, J.A., 2007. The complete ISRM suggested methods for rock characterization, testing and monitoring: 1974-2006. The ISRM Turkish National Group, Ankara.

Utomo, E.P., 2008. Longsoran yang Dipicu Gempa Bumi - Studi Kasus: Longsoran Warungkiara, Sukabumi, Jawa Barat dan Longsoran Raksasa Gowa, Sulawesi Selatan, in: Prosiding Pemaparan Hasil Penelitian Puslit Geoteknologi - LIPI 2008. Bandung, pp. 978–979.

van Bemmelen, R.W., 1949. The geology of Indonesia vol. 1A - general geology of Indonesia and adjacent archipelagoes. Government Printing Office, Hague.

Widiatmaka, Gandasasmita, K., Utomo, W.Y., 2013. An Analysis of Potential Hazard and Risk for Flood and Landslide (Case Study in West Java Province). IPB University.

Widisaputra, R., Zakaria, Z., Sophian, R.I., Iqbal, P., Permana, H., 2020. Pengaruh Beban Gempa terhadap Kestabilan Lereng Tanah Daerah Liwa dan Sekitarnya, Kabupaten Lampung Barat, Lampung. Padjadjaran Geosci. J. 4, 1–9.

Wyllie, D.C., Mah, C.W., 2004. Rock Slope Engineering (Civil and Mining), 4th ed. Spoon Press, London. https://doi.org/10.1201/9781315274980